Minerals Engineering 221 (2025) 109113

Contents lists available at ScienceDirect

Minerals Engineering

journal homepage: www.elsevier.com/locate/mineng

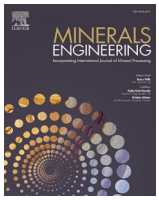

Producing green rutile from secondary ilmenite via hydrogen reduction

William Spencer, Don Ibana, Pritam Singh, Aleksandar N. Nikoloski *

Harry Butler Institute (Centre for Water Energy and Waste), College of Science, Health, Engineering and Education, Murdoch University, 90 South Street, Murdoch, Western Australia 6150, Australia

ARTICLE INFO

Keywords:
Green rutile
Hydrogen reduction
Titanium
Secondary ilmenite
Synthetic rutile

ABSTRACT

The use of coal for ilmenite reduction to produce synthetic rutile is widespread in industry. However, the carbon dioxide emissions associated with coal combustion pose significant environmental concerns. Alternative reductants such as hydrogen have the potential to promote environmentally friendly production of green rutile. This study aimed to assess the technical feasibility of reducing an Australian secondary (weathered) ilmenite using hydrogen, focusing on the effects of reduction temperature and time. The ilmenite was composed of 65 % titanium dioxide, 29 % iron oxide, and 6 % impurities. Samples at each stage of the processing were analysed using X-ray fluorescence spectrometry (XRF) and scanning electron microscopy (SEM). The results revealed that both temperature and time impacted ilmenite reduction, with increasing values of both parameters leading to higher reduction percentages. The maximum reduction percentages were obtained for a reduction time of 240 min at all temperatures, and there was an increase from 62 % at 973 K to 99 % at 1273 K for this reduction time. A reduction percentage of 90 % was obtained at 1273 K with a holding time of 60 min. This study indicates that a minimum temperature of 1073 K is required to achieve a reduction exceeding 90 % for secondary ilmenite. The SEM analysis showed that fine, discrete, metallised iron particles were present on the surface of the reduced secondary ilmenite. The investigation into hydrogen as an alternative reductant demonstrated improved iron–titanium separation in acid leaching compared with the conventional reduction method using coal and resulted in green rutile products with titanium dioxide grades exceeding 96 %, and iron oxide content below 1 %.

1. Introduction

Ilmenite reduction, specifically for secondary ilmenites, plays a critical role in the production of synthetic rutile via the Becher process (Becher et al., 1965). This process relies on coal as the primary reducing agent and is critical for upgrading titanium-bearing minerals into synthetic rutile, a valuable raw material for the titanium pigment industry. Recently, there has been increasing interest in green technologies centred on hydrogen. Using H_2 as a reductant, eliminates CO_2, SO_2, and NO_x emissions and solid carbon waste. Previous studies using H_2 as a reducing agent have mainly focused on primary ilmenites and synthetic ilmenite samples with a low TiO_2 content (Dang et al., 2015; Lu et al., 2016; Lv et al., 2019). These studies have provided valuable insights into the impact of factors such as temperature and time on the reduction kinetics of ilmenite. The suitability of hydrogen reduction for producing synthetic rutile from secondary ilmenites, also known as altered or weathered ilmenites, which are rich in titanium due to natural weathering and iron removal, remains unclear. This study aimed to address this knowledge gap by studying the H_2 reduction of secondary ilmenite while also assessing the quality of the resulting rutile product.

Primary and secondary ilmenites, both with the chemical formula $FeTiO_3$, consist mainly of TiO_2 and FeO, as indicated in Table 1, yet they differ notably in TiO_2 and FeO content. Primary ilmenite can be further classified into two subgroups, primary ilmenites I and II. Ilmenite I contains less gangue than ilmenite II. In contrast to secondary ilmenites, primary ilmenites have a higher FeO content and a denser structure. Secondary ilmenites are classified into two subgroups, secondary ilmenites I and II, based on the TiO_2 content. Secondary ilmenites are formed through the alteration or weathering of primary ilmenite deposits. This alteration process involves the removal of iron due to weathering, erosion, and sedimentation. As a result, secondary ilmenites may have impurities such as alumina, silica, and clays, leading to higher impurity levels.

Past research has explored H_2 reduction in primary and synthetic ilmenites, as shown in Table 2, investigating factors such as impurities, temperature, preoxidation, and hydrogen concentration (Dang et al.,

* Corresponding author.
E-mail address: A.Nikoloski@murdoch.edu.au (A.N. Nikoloski).

https://doi.org/10.1016/j.mineng.2024.109113
Received 25 October 2023; Received in revised form 7 October 2024; Accepted 17 November 2024
Available online 26 November 2024

2015; Lu et al., 2016; Lv et al., 2019). Interpreting such studies is challenging at a fundamental level due to the complex nature of ilmenite types and the variability of ore composition. Preoxidation has positive effect on ilmenite reduction, as shown in Lv's (2019) study using a 30 % H_2 and 70 % Ar mixture at a flow rate of 20 cm^3/min, with reduction temperatures from 1123 K to 1223 K. During preoxidation, $FeO.TiO_2$ transforms into $Fe_2O_3.TiO_2$ (pseudobrookite) and rutile, transitioning from a denser to a porous structure, thereby improving gas reduction. Vijay (1996) studied the reduction of preoxidised ilmenite at a temperature of 1073 K for 2 h, using an equimolar mixture of H_2 and N_2, and a fluidisation velocity of 251.4 cm^3/min to attain higher ilmenite metallisation. In another study conducted by Sargeant (2020) on a 95 % pure ilmenite sample, with an H_2 ratio of 1:1, a reduction temperature of 1273 K and a reduction time of 240 min were utilised to achieve high reduction levels. Lu (2016) study showed that increasing the H_2 to ilmenite ratio resulted in decreased reduction times. Temperature played a critical role in Dang's (2015) study on ilmenite powder reduction, with optimal reduction observed at 1146 K in 28 min and at 1201 K in 14 min using an H_2 and Ar mix at a flow rate of 60 mL/min. Overall, these studies have contributed to the current understanding of the potential of hydrogen to reduce primary ilmenites, but its role in secondary ilmenite reduction remains largely unexplored.

Historically, the term synthetic rutile has been used to describe upgraded ilmenite produced using coal as the main reductant in ilmenite processing. The term green rutile (GR) is used in this paper to differentiate the rutile produced using hydrogen as a reductant.

This study aimed to investigate H_2 gas as a reducing agent for secondary ilmenites, exploring the impact of temperature and time on reduction efficiency and rutile quality. Comprehensive characterisation of both initial secondary ilmenite and resulting products was analysed. The results are relevant to reducing secondary ilmenites in Australia and offer a pathway to produce greener rutile with zero carbon emissions in Australia.

2. Materials and methods

2.1. Preparation of the secondary ilmenite sample

A representative secondary ilmenite sample sourced from Western Australia was used as the feed material in this research. The sample was oven-dried at 363 K for 720 min. The dried secondary ilmenite sample was separated into representative subsamples, each weighing 100 g.

2.2. Reduction of secondary ilmenite

A high-temperature rotating alumina ceramic tube furnace, with a 40 mm outside diameter, 30 mm inside diameter, and 900 mm length, was used for the secondary ilmenite reduction experiments. The furnace tube was rotated at a speed of 10 rpm during the reduction experiments. For each reduction test, a100 g ilmenite sample with 80 % of particles passing 210 μm was used. The sample was placed in the heating zone, as shown in Fig. 1, with thermoblocks used to maintain the sample within the heating zone. The furnace was heated from room temperature (298 K) to the reduction temperature for each test at a rate of 278 K/min. The experiments utilised BOC (British Oxygen Company) scientific grade high-purity hydrogen gas of 99.999 % as a reducing gas, and high-purity N_2 gas of 99.99 % acted as the purging gas. Throughout the experiment, a steady flow of N_2 gas at 1121 cm^3/min (equivalent to 3 mol per hour) was maintained. Once the desired reduction temperature was reached, a consistent flow of H_2 gas at 374 cm^3/min (equivalent to 1 mol of H_2 per hour) was introduced into the tube furnace. After the reduction, the samples were furnace cooled from the reduction temperature to room temperature (298 K) at a rate of 278 K/min.

2.3. Leaching of reduced ilmenite samples

Acid leaching is the second and final stage in the production of GR from ilmenite. A 7 M HCl solution was used as the leaching chemical. ARL-grade chemicals, including hydrochloric acid, copper sulphate, orthophosphoric acid, sulphuric acid, and potassium dichromate, were purchased from Rowe Scientific, Western Australia. The metallic iron content of a sample was measured by reducing the iron oxide to metallic iron, dissolving it, precipitating it as ferrous sulfate, oxidizing it to ferric sulfate, and then titrating it. This wet chemistry method is a reliable and accurate way to measure the metallic iron content of samples (Spencer et al., 2022b; Williams and Anderson, 1922a).

The acid-leaching experiments were carried out on a hot plate using a magnetic stirrer set at 200 rpm and at a temperature of 363 K for 60 min. For leaching, a sample split of 25 g of hydrogen-reduced secondary ilmenite was mixed with 25 mL of 7 M HCl solution. After leaching, the sample was cooled to room temperature and then screened using a 53 μm sieve to separate coarse green rutile particles from undersized iron particles. Fig. 1 provides a flow diagram of the experimental setup for hydrogen reduction of ilmenite and subsequent acid leaching.

2.4. Chemical and mineralogical analysis

Subsamples taken at each stage of the process were milled and then analysed to determine the chemical and mineralogical composition. The determination of metallic iron in each sample was carried out in accordance with the method described in (Williams and Anderson, 1922b). The chemical composition of the green rutile samples was determined by an external laboratory (Bureau Veritas, Canning Vale). The TiO_2 content in the GR samples was analysed using X-ray fluorescence spectrometry (XRF).

A Rigaku SmartLab with a high-resolution X-ray diffractometer was used to characterise feed and product samples. Qualitative and quantitative phase analyses were carried out using Match XRD software, which was used to perform a Rietveld phase analysis.

The surface and morphological features of the samples were characterised using a Joel JCM-7000 Neoscope SEM (scanning electron microscope) with an EDS (energy dispersive spectrometer). For SEM–EDS

Table 1
Key ilmenite groups with their associated titanium minerals, impurities, and physical properties.

Group	Mineral	Phases	TiO_2	FeO	Silicate gangue	Physical property
			%(w/w)			
Primary or natural	Ilmenite I	Ilmenite	> 45 to ≤ 55	>16	<5	Denser
	Ilmenite II	Ilmenite + secondary ilmenite I	> 45 to ≤ 55	>16	≥5 to < 15	Denser
Low-grade/TiO_2	Ilmenite		<50	>16	<15; MnO/MgO < 10	Denser
Weathered Secondary/altered	Ilmenite I	Ilmenite + pseudorutile	>57	<16	<15	Porous
	Ilmenite II	Ilmenite + pseudorutile + rutile	>65 to ≤ 69	<16	<15	Porous
	Pseudorutile	Pseudorutile	~60			Porous
Synthetic minerals	Ilmenite*	Ilmenite	≤55	>16		
	Rutile	Rutile	>88			Porous
Rutile	Rutile	Rutile	>95			

* Ilmenite synthesized from pure TiO_2 and FeO. Note: Unless specified otherwise, the minerals and chemical species mentioned are naturally occurring.

analysis, the unpolished samples were oven-dried and coated with 10 nm carbon. The SEM–EDS was operated in high vacuum mode and at an acceleration voltage range from 5 kV to 30 kV.

2.5. Theory and calculations

The use of coal to reduce oxides, such as iron oxide in ilmenite, is common practice. The three most common forms of iron oxide are hematite (Fe_2O_3), magnetite (Fe_3O_4), and wüstite (FeO). Fig. 2 shows the weight percentage of oxygen present in these iron oxide phases. The reduction of iron oxide in ilmenite occurs in three stages: Fe_2O_3 to Fe_3O_4 to FeO to Fe.

The sample used in this study contained 70 % pseudorutile, 20 % ilmenite, and 10 % rutile, as shown in Fig. 5, with hydrogen reduction mainly targeting pseudorutile and ilmenite. Researchers proposed a two-step process for the conversion of ilmenite to pseudobrookite: first, the oxidation of ilmenite to pseudorutile (Reaction (1), with the subsequent decomposition of pseudorutile into pseudobrookite and rutile occurring at temperatures above 1073 K (Reaction (2) (Teufer and Temple, 1966; Wort, 1980). The pseudobrookite further decomposed into rutile and hematite according to Reaction (3). Reduction of pseudobrookite with H_2 gas occurs as per Reaction 4. Fig. 3 shows Gibbs free energy versus temperature for reactions in the hydrogen reduction of pseudobrookite and ilmenite.

$$Fe_3^{2+}Ti_3O_9 \rightarrow Fe_2^{3+}Ti_3O_9 + 1/2\ Fe_2^{3+}O_3 \quad (1)$$

$$Fe_2^{3+}Ti_3O_9 \rightarrow Fe_2^{3+}TiO_5 + 2TiO_2 \quad (2)$$

$$Fe_2^{3+}TiO_5 \rightarrow TiO_2 + Fe_2O_3 \quad (3)$$

$$Fe_2^{3+}TiO_5 + 3H_2 \rightarrow TiO_2 + 2Fe + 3H_2O \quad (4)$$

Ilmenite reduction using hydrogen gas involves steps outlined in Reactions 5–7. Reaction 8 is a simplified reaction in the reduction of ilmenite using hydrogen (Williams, 1985). HSC software version 9.2 was used to calculate the thermochemical reaction data, including heat of reaction (ΔH), Gibbs free energy (ΔG), entropy (ΔS), and equilibrium constants for selected Reactions, as presented in Table 3.

$$3Fe_2O_3.TiO_2 + H_2 \rightarrow 2Fe_3O_4.TiO_2 + H_2O \quad (5)$$

$$Fe_3O_4.TiO_2 + H_2 \rightarrow 3FeO.TiO_2 + H_2O \quad (6)$$

$$FeO.TiO_2 + H_2 \rightarrow Fe + TiO_2 + H_2O \quad (7)$$

$$FeTiO_3 + H_2 \rightarrow Fe + TiO_2 + H_2O \quad (8)$$

Percentage metallisation and percentage reduction both provide key information regarding ilmenite reduction. The former is a measure of iron present in a metallic state whereas the latter is a measure of oxygen removal from iron oxide. The M (metallisation (%)) in reduced ilmenite (RI) samples was calculated using the following equation:

$$M = \frac{Weightofmetalliciron presentin RI}{Totalweightofiron presentin RI} \times 100 \quad (1)$$

Gupta (2009) pointed out that a linear relationship exists between metallisation and reduction percentages, which can be used to calculate reduction (%) from metallisation (%) via Equation (2) (Gupta, 2009). The reduction (%) values reported in this paper were calculated using this equation:

$$\text{Reduction}\,(\%) = \frac{M + 42.3}{1.4294} \quad (2)$$

TiO_2 recovery was calculated by dividing the mass of TiO_2 (g) in the green rutile sample by the mass of TiO_2 (g) in the secondary ilmenite feed sample and multiplying the result by 100. This yields the TiO_2 recovery percentage, as shown in Equation (3):

$$\text{Recovery}\,(\%) = \frac{WeightofTiO2 presentingreenrutile(g)}{WeightofTiO2 preentinfeedsample(g)} \times 100 \quad (3)$$

3. Results and discussion

3.1. Characterisation of secondary ilmenite sample

Fig. 4 shows the sizing results from cumulative percentage passing vs. sieve size for an initial secondary ilmenite subsample. The sample had a p80 (80 % passing) size of 210 μm. This is a typical size for secondary ilmenites found in beach deposits but slightly coarser than some ilmenite deposits in Australia. The head assay results for the secondary

Table 2
Hydrogen reduction process for various ilmenites and the corresponding final products.

Type of ilmenite	Particle size	Main minerals	Major impurities	Reduction			Final product	References
Feed	μm	Phases	%(w/w)	Equipment	Reductant	Phases		
Panzhihua ilmenite concentrate	26–104	Magnesian ilmenite ((Fe, Mg)TiO_3) and titanomagnetite (Fe_2TiO_4–Fe_3O_4).	Mg, Al + Si > 5 %	TGA	H_2–Ar/H_2	Fe, pseudo-brookite, rutile	Reduced ilmenite	(Lu et al., 2016)
Panzhihua low-grade ilmenite	40.87	Magnesian ilmenite ((Fe, Mg)TiO_3).	Mg < 10 %, Al + Si < 5 %	TGA	H_2–Ar	Fe, Mg ilmenite, rutile	Reduced ilmenite	(Dang et al., 2015)
Preoxidised Panzhihua raw ilmenite concentrate	74	Magnesian ilmenite ((Fe, Mg)TiO_3).	Mg < 5 %, Al + Si < 5 %	TGA	H_2–Ar	Fe, Mg ilmenite, rutile	Reduced ilmenite	(Lv et al., 2019)
Preoxidised raw Quilion ilmenite	53–250		Al + Si < 5 %	Fluidised bed	H_2–N_2		Reduced ilmenite	(Vijay et al., 1996)
Synthetic ilmenite	45	Ilmenite ($FeTiO_3$)		Quartz flow-through reactor	H_2	Fe, rutile	Reduced ilmenite	(Zhao and Shadman, 1991)
Preoxidised natural (primary) ilmenite	90–300	Ilmenite ($FeTiO_3$)	Al + Si < 5 %	Fluidised bed	H_2–H_2O		Reduced ilmenite	(Grey et al., 2007)
Preoxidised ilmenite pellets		Ilmenite ($FeTiO_3$), haematite (Fe_2O_3), armalcolite, pseudorutile ($Fe_2Ti_3O_9$), and rutile (TiO_2).	Mg < 5 %, Al + Si < 5 %	TGA	H_2–CO	Fe, M_2O_3, M_3O_5, rutile	Reduced ilmenite	(Lobo et al., 2016)
Western Australian weathered secondary ilmenite	53–425	Ilmenite ($FeTiO_3$), pseudorutile ($Fe_2Ti_3O_9$), and rutile (TiO_2)	Al + Si < 5 %	Lab kiln	H_2–N_2	Fe, Ti_2O_3, rutile	Rutile*	This work

* In the current study, the reduced ilmenite underwent acid leaching to generate green rutile.

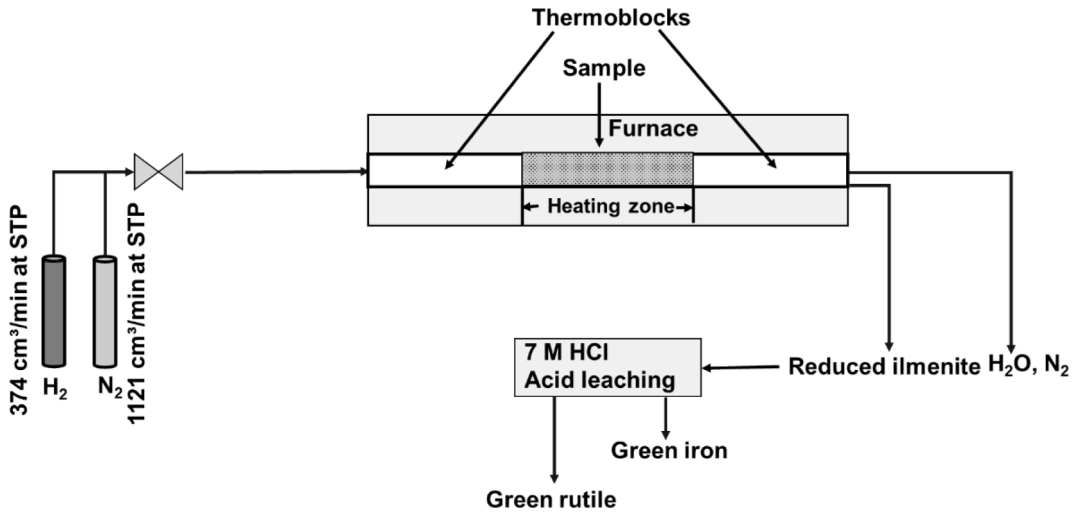

Fig. 1. Schematic diagram of the hydrogen reduction and acid-leaching experiment, showing the steps involved in the process.

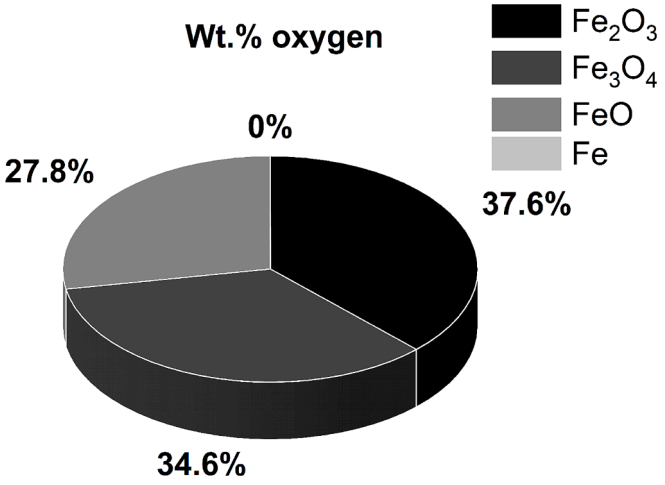

Fig. 2. Distribution of oxygen (percentage by weight) in iron oxide phases.

ilmenite sample are presented in Table 4. The sample contained 65 % TiO_2, 30 % Fe_2O_3, and other oxides in minor amounts.

Fig. 5 shows the XRD spectrum for the secondary ilmenite sample and the phase composition calculated using Match XRD phase software and the Rietveld refinement technique. The results indicated that the sample was 70 % pseudorutile, 20 % ilmenite, and 10 % rutile. The ilmenite used in this study was secondary or altered (weathered) ilmenite, which has a higher titanium oxide content ($TiO_2 > 61$ %) then primary ilmenites due to the presence of pseudorutile phases. Primary ilmenites contain approximately equal amounts of TiO_2 and Fe_2O_3. The weathering of ilmenite ores results in the removal of iron from the grains, leading to an increase in titanium content and the formation of pseudorutile phases with a high titanium content.

3.2. Reduction of secondary ilmenite

The reduction of secondary ilmenite using hydrogen was calculated according to its metallisation (%) (Equation (1), which remains one of the principal quantitative reduction assessment methods. Fig. 6 presents the results of the reduction of secondary ilmenite using H_2 gas. The reduction percentages were found to be 62 % at 973 K, 90 % at 1073 K, 93 % at 1123 K, 97 % at 1173 K, and 99 % at 1273 K, after a reduction

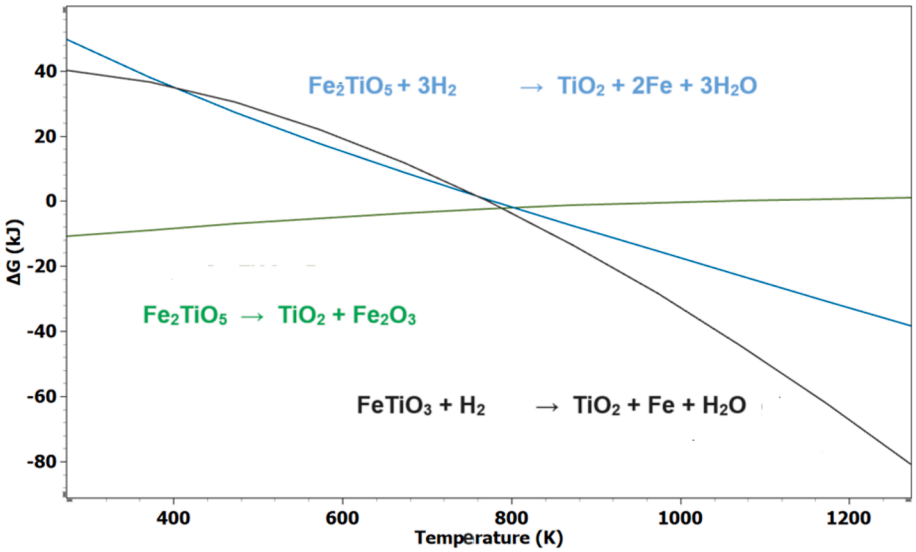

Fig. 3. Gibbs free energy vs. temperature for reactions in hydrogen reduction of secondary ilmenite, calculated using HSC software.

Table 3
Thermochemical reaction data for selected Reactions.

	Reaction (3)				Reaction (4)				Reaction (8)			
T	ΔH	ΔS	ΔG	Log K	ΔH	ΔS	ΔG	Log K	ΔH	ΔS	ΔG	Log K
K	kJ	J/K	kJ		kJ	J/K	kJ		kJ	J/K	kJ	
273.2	−15.8	−18.2	−10.9	2.1	84.4	126.7	49.8	−9.5	46.4	22.6	40.2	−7.7
373.2	−16.2	−19.3	−9.0	1.3	79.8	112.3	37.9	−5.3	55.1	49.8	36.5	−5.1
473.2	−15.8	−18.5	−7.1	0.8	75.0	101.0	27.2	−3.0	64.9	73.0	30.4	−3.4
573.2	−15.0	−17.0	−5.3	0.5	70.5	92.4	17.6	−1.6	75.4	93.0	22.0	−2.0
673.2	−13.7	−14.9	−3.7	0.3	66.5	85.9	8.7	−0.7	86.4	110.8	11.8	−0.9
773.2	−11.9	−12.4	−2.3	0.2	63.2	81.3	0.3	0.0	98.0	126.9	−0.1	0.0
873.2	−9.3	−9.3	−1.2	0.1	60.7	78.3	−7.6	0.5	110.3	141.8	−13.5	0.8
973.2	−5.8	−5.5	−0.5	0.0	59.6	77.1	−15.4	0.8	123.4	156.0	−28.4	1.5
1073.2	−5.2	−4.8	0.0	0.0	60.0	77.4	−23.1	1.1	137.4	169.7	−44.7	2.2
1173.2	−5.1	−4.7	0.5	0.0	58.5	76.1	−30.8	1.4	150.6	181.5	−62.3	2.8
1273.2	−5.1	−4.8	0.9	0.0	57.3	75.2	−38.4	1.6	164.1	192.5	−81.0	3.3

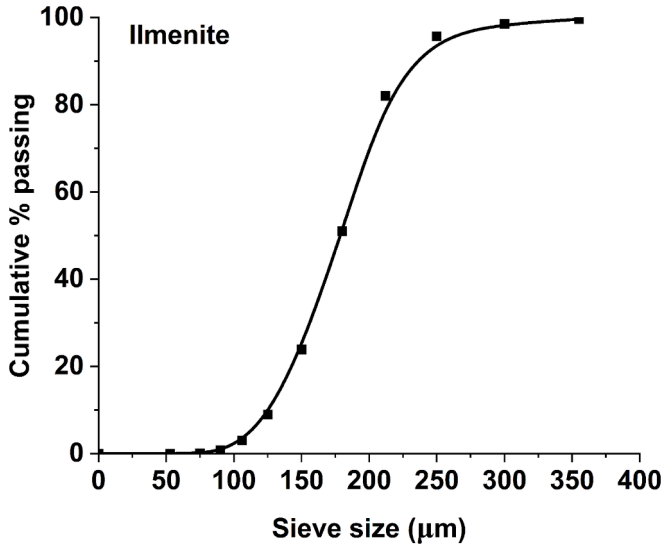

Fig. 4. A typical particle size distribution curve for the secondary ilmenite sample.

time of 240 min. The low reduction percentages at 973 K were explained by the fact that there was insufficient conversion of pseudorutile to pseudobrookite at this temperature, which affected H2 reduction as evidenced by the reduction curve separating from the rest. These findings demonstrated that reduction efficiency increased with higher temperatures. Furthermore, a reduction percentage of 90 % was achieved at 1273 K in a reduced timeframe of 60 min. These results indicate that it is feasible to achieve a reduction greater than 90 % by using a higher temperature for a shorter reduction time.

Fig. 6 shows the results of the percentage of secondary ilmenite reduction and the quantity of H_2 gas used in the reduction process. The outcomes underscore the economic advantage from requiring less H_2 gas (1 mol) to achieve 90 % reduction at higher temperatures for shorter reduction times compared to reduction at lower temperatures. Importantly, lower temperatures need longer reduction periods, resulting in increased H_2 gas requirements. These findings highlight the importance of optimizing process parameters, such as temperature and reduction time, to achieve a desirable equilibrium between elevated reduction percentages and minimised H_2 gas usage. This optimisation is crucial to ensure cost-effectiveness in the secondary ilmenite reduction process.

Fig. 7 shows the XRD spectra for the hydrogen-reduced samples. In these XRD spectra, three phases can be observed. The main diffraction peak for metallic iron (Fe) appeared at a 2θ angle of 44.78° with a small peak at 65.18°. Structural factor calculations were performed for metallic iron and these peaks are related to a cubic system with cell indices of *hkl* 110 and *hkl* 200.

As shown in Fig. 7, the prominent peak of rutile appeared at a 2θ angle of 27.38°. This peak signifies the crystallographic orientation and characteristic lattice structure of rutile. In addition to the main peak, there were several minor peaks observed within the 2θ range of 30° to 75°, indicating the presence of rutile in the sample. Interestingly, the XRD spectra also exhibited the presence of another titanium phase, namely, Ti_2O_3.The formation of this trivalent titanium phase was observed to occur for lower reduction temperatures rather than for higher-temperature reduction processes. In conventional coal-based ilmenite reduction processes, the presence of Ti_2O_3 is typically observed at temperatures exceeding 1373 K, and can serve as an indicator that the kiln is operating within the desired temperature range to achieve the intended reduction of ilmenite. The development of Ti_2O_3 during ilmenite reduction using hydrogen is depicted in Reactions 9 and 10. The Ti_2O_3 phase, known for its thermal instability, can transform into the rutile phase, even in the presence of small amounts of oxygen, as per Reaction 11. The XRD spectra validate the oxidation of the Ti_2O_3 phase at higher temperatures in the presence of an N_2–H_2 gas mixture. This study supports the evidence from a previous study that nitrogen gas aids in the transformation of Ti_2O_3 to TiO_2 (Yu and Chen, 2010).

$$4FeTiO_3 + 6H_2 \rightarrow 4Fe + 2Ti_2O_3 + 6H_2O \quad (9)$$

$$4TiO_2 + 2H_2 \rightarrow 2Ti_2O_3 + 2H_2O \quad (10)$$

$$2Ti_2O_3 + O_2 \rightarrow 4TiO_2 \quad (11)$$

According to the thermochemical reaction data shown in Table 5, Reaction 9 becomes thermochemically more favourable above 1073 K, where ΔG turns negative and the equilibrium constant (K) indicates a stronger driving force towards product formation at higher temperatures. Reaction 10 continues as unfavourable, though decreasing ΔG reflects reduced thermochemical resistance at higher temperatures. Reaction 11 presents strong spontaneity across the entire temperature range. The present results are in agreement with Zhao and Shadman (1991) who investigated the hydrogen reduction of rutile at a temperature of 1287 K, revealing that the reduction of TiO_2 does not occur to a

Table 4
Chemical composition of secondary ilmenite sample.

Oxide	TiO_2	Fe_2O_3	MnO	Al_2O_3	SiO_2	V_2O_5	MgO	Cr_2O_3	Others
Wt. %	65.41	30.32	1.10	1.05	0.66	0.37	0.32	0.25	0.48

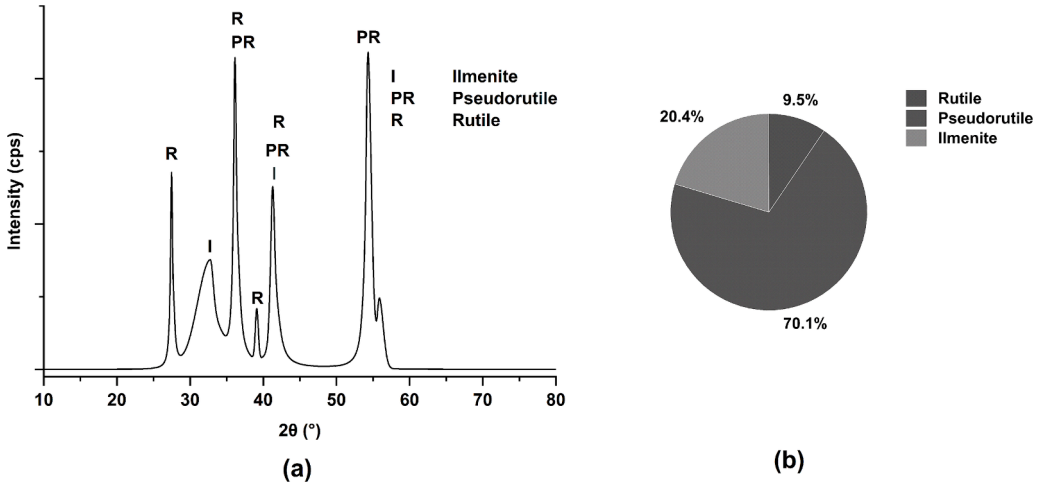

Fig. 5. Mineralogy of secondary ilmenite sample: (a) XRD spectrum and (b) XRD phase composition (weight %).

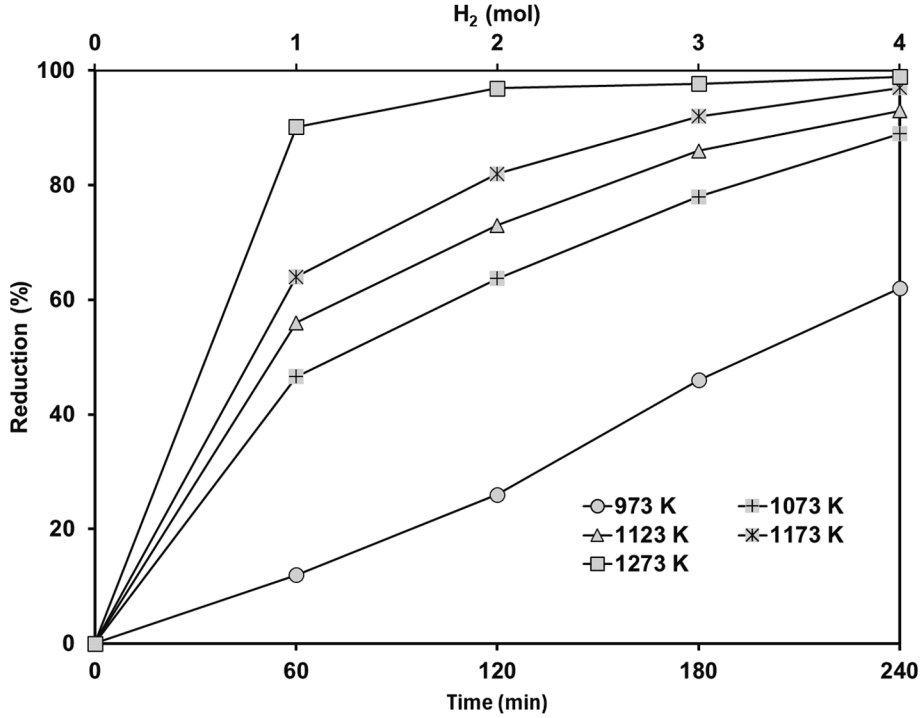

Fig. 6. Reduction percentage of the secondary ilmenite sample reduced by H_2 at different temperatures and flow rates.

significant extent until iron metallisation is completed. High concentration of water vapour within the TiO_2 pores inhibits reduction; however, as the metallisation of iron nears completion, this inhibition diminishes, facilitating the initiation of TiO_2 reduction, particularly at elevated temperatures (Zhao and Shadman, 1991).

SEM images of the RI samples are shown in Fig. 8. It can be observed that metallic iron migrated to the surface, appearing as discrete fine particles (Fig. 8c, d). The iron particles closer to the surface are more likely to migrate, whereas those inside may not have the opportunity to do so. EDS analysis suggested that these particles had an iron content of $>$ 98 %. The morphology of the RI particles showed no visible sintering. However, the size of the iron particles appeared to increase as the temperature decreased. Fig. 9 shows secondary ilmenite reduced with coal at 1373 K in the conventional Becher process. The difference in appearance of particle size was clearly visible when compared with H_2-reduced samples. A possible explanation for this might be that ilmenite reduction using coal is conducted at higher temperatures, as previous studies found that temperature had a major effect on the formation of iron particles on the ilmenite surface (Ranganathan et al., 2012; Spencer et al., 2022a).

3.3. *Effect of reduction parameters*

The effect of reduction parameters, namely, temperature and time, on the hydrogen reduction of secondary ilmenite (as depicted in Fig. 6) indicated that temperatures at the hight end of the range 973 K to 1273 K led to increased percentages of ilmenite reduction. A strong relationship between reduction percentage and both temperature and time is evident from the figure. Notably, at the highest temperature of 1273 K and a maximum reduction time of 240 min, almost complete reduction of ilmenite (99 %) was achieved. It was observed that the reduction rate was more rapid during the initial 60 min at elevated temperatures and

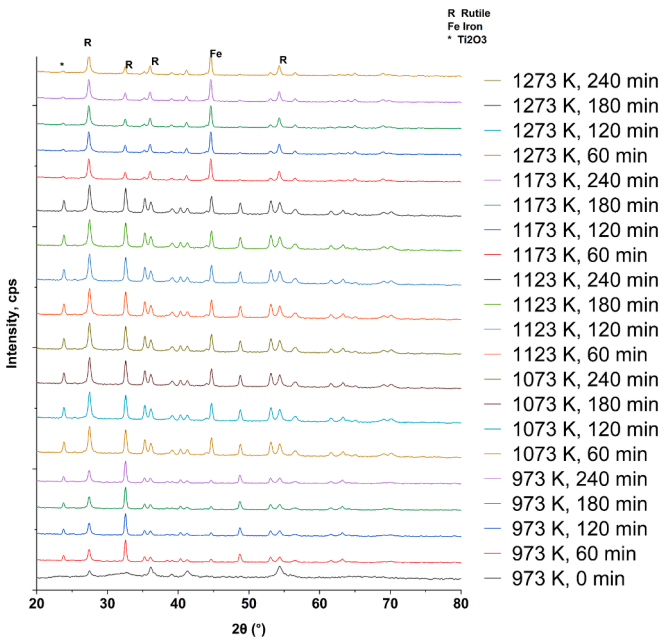

Fig. 7. XRD spectra of RI samples.

slowed down after the sample had achieved 90 % reduction.

The results indicated that increasing the reduction time improved the conversion of Fe^{3+} to Fe, resulting in a high reduction (%), although this was not as strong as the impact of increasing the temperature. A possible explanation for this is that at lower temperatures, reduction reaction kinetics are slower and therefore, additional time is required to complete the reduction. At higher temperatures, however, reaction kinetics are faster, and a shorter time could be sufficient. Achieving over 90 % metallisation in this study corroborates the findings of Zhao and Shadman (1991), confirming the effective reduction of iron in ilmenite. The results indicate improved reduction kinetics at elevated temperatures, with markedly shorter metallisation times at 1287 K.

The results support a previous study which showed complete reduction of a synthetic ilmenite sample with lower titanium content was achieved using H_2 at a temperature of 1145 K (Baysal et al., 2021). However, this finding is contrary to a study involving lunar ilmenites, which observed incomplete reduction at 1373 K (Sargeant et al., 2020). This inconsistency can possibly be attributed to the influence of the surface area and internal porosity of the ilmenite samples on the extent of reduction. This finding broadly supports the observations from other studies in this area which linked surface area and porosity to ilmenite reduction (Spencer et al., 2022b). The findings of the study reported in this paper indicated that ilmenite samples characterised by high surface area and high internal porosity displayed a higher percentage of reduction.

3.4. Replicate tests and statistical analysis

Table 6 presents the results of five replicate tests conducted to assess the reduction percentages at various temperatures for both the original and replicate tests. The mean reduction percentages across all temperatures indicate a consistent trend, with values ranging from 72.4 % at 973 K to 95.2 % at 1273 K. The standard deviation values for these replicate tests, which are relatively low (± 0.3 to ± 0.5), suggest minimal variability between the observed test results and high reproducibility, which supports the reliability of the reported findings.

3.5. Production of green rutile

GR samples were produced by acid leaching of the reduced ilmenite and chemical analysis of the GR was performed at Bureau Veritas in accordance with Australian and international analytical methods. The samples were analysed using XRF for titanium, iron, and the other impurities in Table 4. Fig. 10a and b show the results of the chemical analysis of green rutile produced from secondary ilmenite reduced with H_2 at different temperatures. The results indicate that TiO_2 content increased with increased reduction temperature. This is because higher temperatures lead to higher reduction percentages and make it easier to leach iron from the ilmenite grains. Fig. 10b shows that samples reduced at high temperatures had a low Fe_2O_3 content of less than 1 % after leaching for 250 min, whereas samples reduced at the lowest temperature had a Fe_2O_3 content of greater than 1 %. The results for all except the lowest temperature indicated a significant upgrade of titanium in the samples, with only a small percentage of iron remaining. The iron content in the GR was much lower than in natural rutile, and the TiO_2 content was higher than that typically found in synthetic rutile (94 % or lower) (Spencer et al., 2022). The lower titanium in synthetic rutile is typically due to impurity elements such as iron, manganese, alumina, silica, magnesium, chromium, and others. In the GR samples produced in the present study, these elements were present at maximum non-iron impurity levels of less than 2 %.

In the conventional Becher process, the use of coal as a reducing agent poses significant challenges for the removal of impurities during aeration leaching (Becher et al., 1965). The impurities present in coal contribute to the formation of phases such as fayalite, M_2O_3, M_3O_5, and M_3O_7 compounds due to the presence of elements such as alumina, silica, manganese, chromium, and magnesium. A comparative investigation focusing on ilmenite of similar quality as the sample in the study reported in this paper that was subjected to coal-based reduction and subsequent acid leaching, highlighted the ineffectiveness of acid leaching in removing these impurities (Spencer et al., 2022b). This resulted in the production of synthetic rutile with a TiO_2 grade of

Table 5
Thermochemical reaction data for Reactions 9 to 11.

	Reaction (9)				Reaction (10)				Reaction (11)			
T	ΔH	ΔS	ΔG	Log K	ΔH	ΔS	ΔG	Log K	ΔH	ΔS	ΔG	Log K
K	kJ	J/K	kJ		kJ	J/K	kJ		kJ	J/K	kJ	
273.2	439.4	161.5	395.3	−75.6	254.0	71.1	234.6	−44.9	−737.2	−158.2	−693.9	132.7
373.2	472.8	265.1	373.9	−52.3	252.3	65.7	227.8	−31.9	−737.4	−159.0	−678.1	94.9
473.2	514.1	362.2	342.7	−37.8	254.4	70.1	221.2	−24.4	−741.4	−167.9	−662.0	73.1
573.2	556.4	443.2	302.3	−27.6	254.9	71.0	214.2	−19.5	−743.7	−172.2	−645.0	58.8
673.2	601.4	515.6	254.3	−19.7	255.7	72.4	207.0	−16.1	−746.3	−176.4	−627.6	48.7
773.2	649.1	581.6	199.4	−13.5	256.9	73.9	199.7	−13.5	−749.0	−180.2	−609.7	41.2
873.2	699.5	642.9	138.1	−8.3	258.2	75.5	192.2	−11.5	−751.9	−183.6	−591.5	35.4
973.2	753.4	701.3	70.9	−3.8	259.6	77.1	184.6	−9.9	−754.7	−186.7	−573.0	30.8
1073.2	810.9	757.5	−2.1	0.1	261.2	78.6	176.8	−8.6	−757.6	−189.5	−554.2	27.0
1173.2	865.5	806.2	−80.3	3.6	263.0	80.2	168.9	−7.5	−760.5	−192.1	−535.1	23.8
1273.2	921.1	851.8	−163.4	6.7	264.8	81.7	160.8	−6.6	−763.4	−194.5	−515.8	21.2

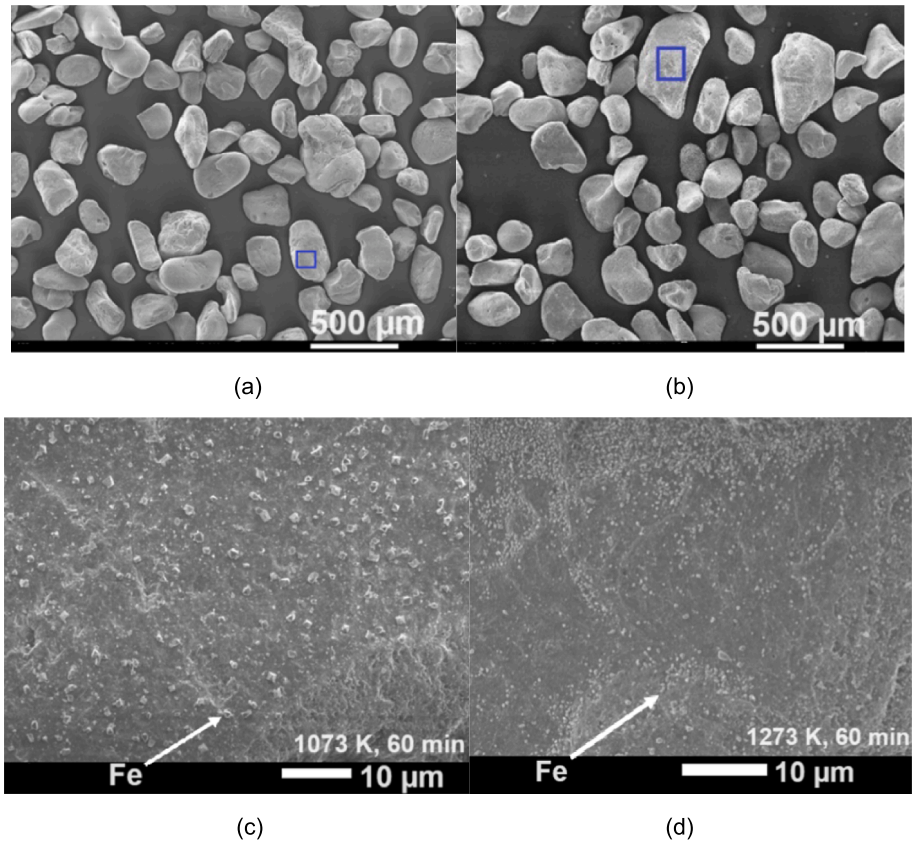

Fig. 8. SEM images of RI samples: (a, b) taken at 500 µm, (c, d) taken at 10 µm.

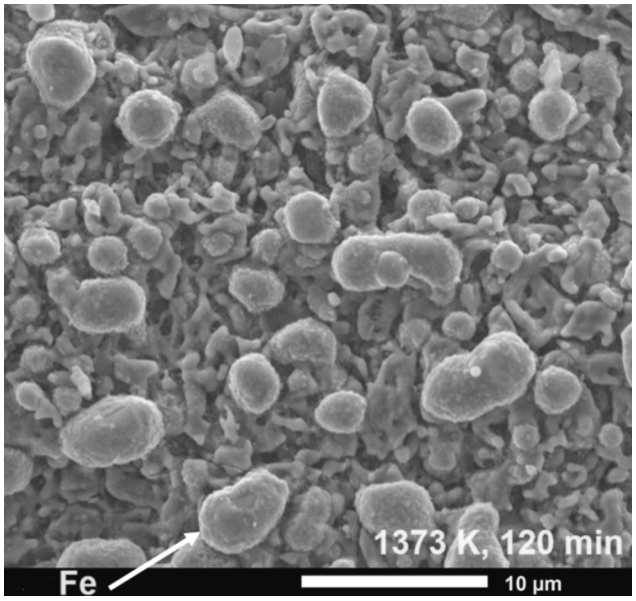

Fig. 9. SEM image of secondary ilmenite sample reduced with coal, taken at 10 µm.

approximately 92 %. In contrast, the use of pure H_2 gas as a reducing agent in this study resulted in minimal to no formation of these complex oxides and a substantial reduction in impurities following acid leaching.

SEM images of the GR samples are presented in Fig. 11. The images at 500 µm indicate a rounded, subrounded, or subangular particle shape with a clean surface. Closer inspection of the samples at higher magnifications shows increased particle porosity due to the removal of iron and other impurities, such as manganese, magnesium, aluminium, and silica by acid leaching.

4. Conclusions

Coal is traditionally used as a reductant in the processing of ilmenites to produce synthetic rutile. However, there is growing concern relating to the greenhouse gases produced during the reduction of ilmenite using coal. This study investigated the use of hydrogen gas as a reductant for secondary ilmenites with the aim of achieving zero carbon emissions in the reduction process while as a minimum maintaining recovery and grade of the synthetic rutile product.

The experimental results highlighted that temperature and time are both critical parameters in the reduction of secondary ilmenites using hydrogen gas. It was found that higher reduction percentages can be achieved with either higher temperatures and shorter reduction times or lower temperatures and longer reduction times. However, the effect of temperature was more pronounced than that of reduction time. A minimum temperature of 1073 K is required to achieve above 90 % reduction of secondary ilmenite.

The research presented here demonstrates that hydrogen gas could be a suitable reductant for secondary ilmenites and, in addition, could yield greater ilmenite reduction rates than coal while using lower reduction temperatures. Hydrochloric acid leaching of hydrogen-reduced ilmenite samples resulted in good separation of TiO_2 from impurities such as iron, manganese, magnesium, alumina, and silica. A notable achievement of this research was the production of GR samples with a TiO_2 grade exceeding 96 %. This was mostly due to a considerable reduction in iron levels, by approximately 96–98 %. However, the levels of other impurities in the original secondary ilmenite, including manganese, magnesium, alumina, and silica, were removed during the leaching step. Chemical and mineralogical examination of the resulting green rutile samples showed that the TiO_2 grade ranged between 96 %

Table 6
Reduction percentages and statistical analysis for original and replicate tests.

Test type	Time (min)	Reduction % at 973 K	Reduction % at 1073 K	Reduction % at 1123 K	Reduction % at 1173 K	Reduction % at 1273 K
Original	120	72.8	87.7	90.2	93.3	95.4
Replicate	120	72.1	88.3	90.7	92.7	95.0
Mean (μ)		72.4	88.0	90.4	93.0	95.2
SD (σ)		± 0.5	± 0.5	± 0.4	± 0.4	± 0.3

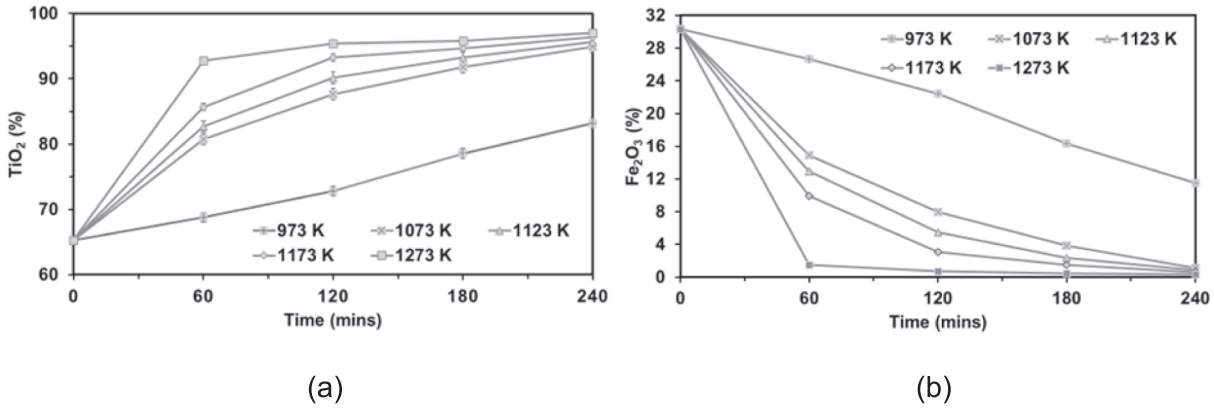

Fig. 10. Results of chemical analysis of green rutile produced from secondary ilmenite reduced with H_2 at different temperatures: (a) TiO_2 (%) vs. time; (b) Fe_2O_3 (%) vs. time.

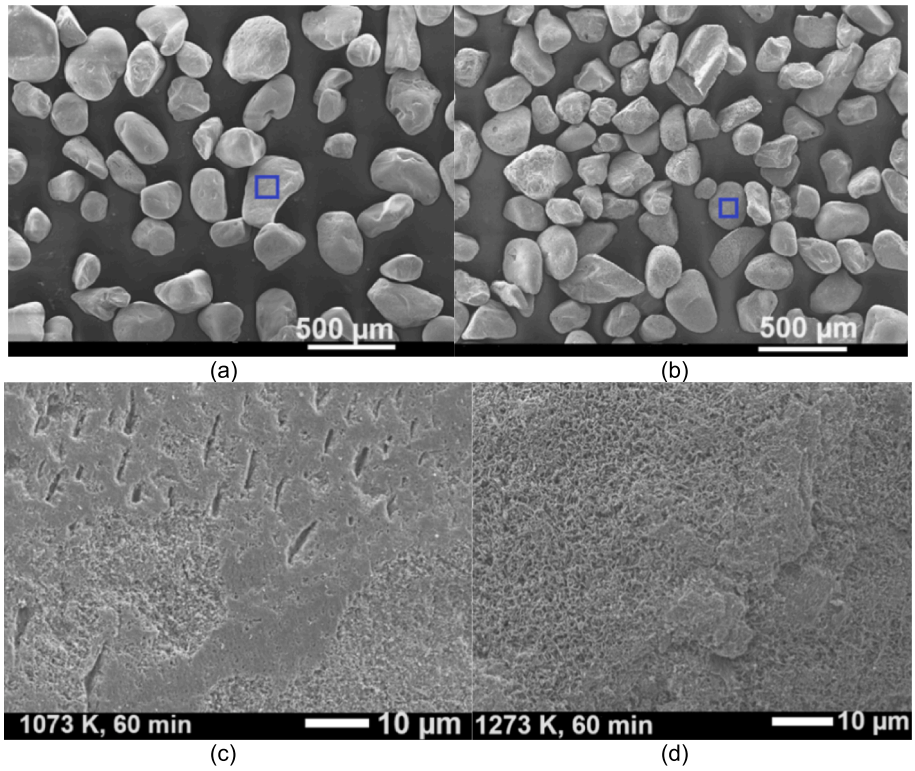

Fig. 11. SEM micrographs of GR samples. (a, b) GR sample at 500 μm, (c, d) GR sample at 10 μm.

and 98 %, with Fe_2O_3 less than 1 %. This compares favourably with TiO_2 grades in synthetic rutile which are typically below 94 %. This study shows that the use of hydrogen gas to produce green rutile results in a higher TiO_2 grade and with zero carbon dioxide emissions.

CRediT authorship contribution statement

William Spencer: Writing – review & editing, Writing – original draft, Methodology, Investigation, Funding acquisition, Formal analysis, Data curation, Conceptualization. **Don Ibana:** Writing – review & editing, Validation, Supervision, Investigation, Conceptualization. **Pritam Singh:** Writing – review & editing, Validation, Supervision,

Investigation, Data curation. **Aleksandar N. Nikoloski:** Writing – review & editing, Writing – original draft, Visualization, Validation, Supervision, Resources, Project administration, Methodology, Investigation, Funding acquisition, Formal analysis, Data curation, Conceptualization.

Declaration of competing interest

The authors declare that they have no known competing financial interests or personal relationships that could have appeared to influence the work reported in this paper.

Acknowledgement

Our sincere thanks to Dennis Plester for kindly supplying the ilmenite samples. The authors acknowledge the facilities and the scientific and technical assistance of Microscopy Australia at the Centre for Microscopy, Characterisation & Analysis, The University of Western Australia, a facility funded by the University, State and Commonwealth Governments.

Data availability

The data that has been used is confidential.

References

Baysal, Z., Kirchner, J., Mehne, M., Kureti, S., 2021. Study on the reduction of ilmenite-type FeTiO3 by H2. Int. J. Hydrogen Energy 46 (5), 4447–4459.

Becher, R., Canning, R., Goodheart, B., Uusna, S., 1965. A new process for upgrading ilmenitic mineral sands. In *Australasian Inst Mining Met Proc* 21–44.

Dang, J., Zhang, G.-H., Chou, K.-C., 2015. Kinetics and mechanism of hydrogen reduction of ilmenite powders. J. Alloy. Compd. 619, 443–451.

Grey, I., McDonald, K., Fisher-White, M., de Vries, M., 2007. Hydrogen reduction of preoxidised ilmenite in fluidised bed and packed bed reactors. Mineral Processing and Extractive Metallurgy 116 (4), 209–216.

Gupta R., *Theory and laboratory experiments in ferrous metallurgy*. 2009, PHI Learning Pvt. Ltd.

Lobo, S., Kolbeinsen, L., Seim, S., 2016. Reduction of Norwegian and Indian ilmenite with carbon monoxide and hydrogen gas blends. Can. Metall. Q. 55 (4), 455–462.

Lu, C.-Y., Zou, X.-L., Lu, X.-G., Xie, X.-L., Zheng, K., Wei, X., Cheng, H.-W., Li, G.-S., 2016. Reductive kinetics of Panzhihua ilmenite with hydrogen. Trans. Nonferrous Met. Soc. Chin. 26 (12), 3266–3273.

Lv, W., Lv, X., Xiang, J., Hu, K., Zhao, S., Dang, J., Han, K., Song, B., 2019. Effect of preoxidation on the reduction of ilmenite concentrate powder by hydrogen. Int. J. Hydrogen Energy 44 (8), 4031–4040.

Ranganathan, S., Bhattacharyya, K.K., Ray, A.K., Godiwalla, K.M., 2012. Investigations on the reduction and growth of particles of iron from ilmenite ore. Mineral Processing and Extractive Metallurgy 121 (1), 55–63.

Sargeant, H.M., Abernethy, F.A.J., Barber, S.J., Wright, I.P., Anand, M., Sheridan, S., Morse, A., 2020. Hydrogen reduction of ilmenite: towards an in situ resource utilization demonstration on the surface of the Moon. Planet. Space Sci. 180, 104751.

Spencer, W., Ibana, D., Singh, P., Nikoloski, A.N., 2022a. Biofuels as renewable reductants for the processing of ilmenite to produce synthetic rutile. Miner. Eng. 187, 107808.

Spencer, W., Ibana, D., Singh, P., Nikoloski, A.N., 2022b. Effect of ilmenite properties on synthetic rutile quality. Miner. Eng. 177, 107365.

Teufer, G., Temple, A., 1966. Pseudorutile—a new mineral intermediate between ilmenite and rutile in the N alteration of ilmenite. Nature 211 (5045), 179–181.

Vijay, P., Venugopalan, R., Sathiyamoorthy, D., 1996. Preoxidation and hydrogen reduction of ilmenite in a fluidized bed reactor. Metall. Mater. Trans. B 27, 731–738.

Williams, R.J., 1985. Oxygen extraction from lunar materials: An experimental test of an ilmenite reduction process. In: In *Lunar Bases and Space Activities of the 21st Century*, p. 551.

Williams, C.E., Anderson, A.E., 1922. The determination of metallic iron in sponge iron. Ind. Eng. Chem. 14 (11), 1057–1059.

Wort, M.J., 1980. Magnetic and other properties of detrital ilmenite and pseudorutile. University of London.

Yu, J., Chen, Y., 2010. One-dimensional growth of TiO2 nanorods from ilmenite sands. J. Alloy. Compd. 504, S364–S367.

Zhao, Y., Shadman, F., 1991. Reduction of ilmenite with hydrogen. Ind. Eng. Chem. Res. 30 (9), 2080–2087.